$\gamma d \to \pi^0 d$ reaction near the threshold of η production

A. E. Kudryavtsev,[1] V. E. Tarasov,[1,*] I. I. Strakovsky,[2,†] Y. Ilieva,[2,‡] and W. J. Briscoe[2,§]
[1]*Institute of Theoretical and Experimental Physics, 25 Bolshaya Cheremushkinskaya Street, Moscow 117259, Russia*
[2]*Center for Nuclear Studies, Department of Physics, The George Washington University, Washington, DC 20052*
(Received 12 August 2004; published 30 March 2005)

We consider the reaction $\gamma d \to \pi^0 d$ in a wide energy range around and above the η-meson photoproduction threshold at backward c.m. angles of the outgoing pions. Our theoretical analysis is motivated by the recent measurements of the CLAS Collaboration at Jefferson Lab, where this kinematical region of the reaction has been thoroughly studied for the first time and an enhancement in the energy dependence of the differential cross section in the region of $E_\gamma \sim 600$–800 MeV has been observed. Our preliminary and qualitative analysis, based on single- and double-scattering diagrams, shows that the observed structure can be explained by the contribution of the double-scattering diagram with intermediate production of the η meson. The effect, to a considerable extent, is due to the contribution of the $N(1535)$ resonance to the amplitudes of subprocesses on the nucleons.

DOI: 10.1103/PhysRevC.71.035202 PACS number(s): 13.60.Le, 14.20.Gk, 25.20.Dc

I. INTRODUCTION

The reaction of coherent photoproduction of the π^0 meson on the deuteron,

$$\gamma d \to \pi^0 d, \tag{1}$$

has recently been studied [1] at Jefferson Lab using the CLAS detector. The experiment was carried out for a wide range of photon energies $E_\gamma = 0.5$–2.0 GeV at large c.m. scattering angles of the outgoing pions. A new phenomenon was observed.

The process of pion photoproduction on the nucleon $\gamma p \to \pi N$ has been theoretically investigated over a long period of time (see, for example, Refs. [2–5]). Reaction (1) on the deuteron also has been considered in a number of papers [6–8]. A through review of pion photoproduction reactions induced in few-body systems can be found in Ref. [9]. During the past few years, η-photoproduction processes have also been actively studied (see, for example, Refs. [10,11] for $\gamma p \to \eta p$, [8,12] for $\gamma d \to \eta d$, and [13] for η photoproduction on light nuclei).

The study of meson-photoproduction processes on a deuteron target provides information about the underlying reaction mechanisms on few-body systems. Our project has been motivated by a special interest in role of intermediate particles in reaction (1).

In the 1970s, the contribution of intermediate particles and resonances to the differential cross section in backward πd elastic scattering was theoretically discussed in Ref. [14]. It has been predicted that the contribution of intermediate particles, formed in a two-step process, should manifest itself as a maximum in the energy dependence of the backward differential cross section around the corresponding thresholds. Such an effect, associated with intermediate η-meson production, was confirmed by several independent measurements of backward πd elastic scattering [15].

The preliminary CLAS photoproduction data [1] give for the first time clear evidence for the intermediate η-meson effect. A visible excess of events in the region $E_\gamma \sim 600$–800 MeV, around the η-photoproduction threshold, survives in the energy dependence of the differential cross section at large c.m. scattering angles, $\cos\theta < -0.6$. The observed effect becomes more pronounced as the scattering angle increases. This behavior was also seen in a previous measurement of reaction (1) [16] in which a small structure was observed in the excitation function at $\cos\theta = -0.64$ (the maximum scattering angle of this experiment). Reaction (1) was also theoretically considered earlier (see, for example, Ref. [4]) in the framework of a single- and double-scattering approach without consideration of the intermediate η meson. A reasonable theoretical description of the previous data [16] was achieved without the necessity of inclusion of the "η effect" [4] at low momentum transfer.

The aim of the present paper is the theoretical study of reaction (1) at large pion production angles. Our principal interest is the contribution of the intermediate η meson to the differential cross section and whether it can explain the structure in the differential cross section that has been observed in a recent CLAS experiment [1]. We shall use the standard approach based on single- and double-scattering amplitudes. The main contribution to the total amplitude at large angles is expected to come from the double-scattering terms. We shall consider photon energies far from the πd threshold, say $500 < E_\gamma < 1000$ MeV, where the influence of the intermediate $N(1535)$ resonance and the η-meson effect should be important, and it is possible to neglect the excitation of the $\Delta(1232)$ isobar in the intermediate state. Thus, we construct the total reaction amplitude from terms, expected to be essential, with approximate values of the parameters. In this paper, although we do compare our predictions with the data qualitatively and present all the details of our treatment, we do not attempt a detailed description of the CLAS data; we leave this task for forthcoming papers from the CLAS Collaboration.

*Electronic address: tarasov@heron.itep.ru
†Electronic address: igor@gwu.edu
‡Electronic address: jordanka@jlab.org
§Electronic address: briscoe@gwu.edu

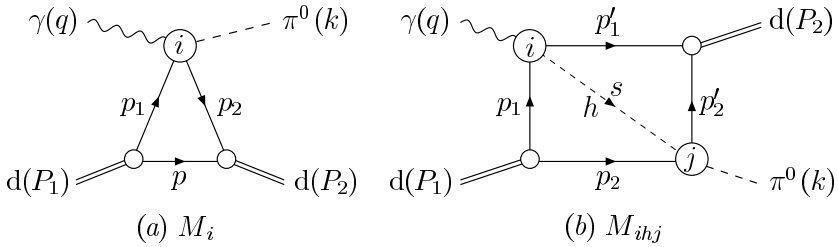

FIG. 1. Feynman diagrams for the $\gamma d \to \pi^0 d$ reaction: (a) single scattering and (b) double scattering.

This paper is organized as follows. In Sec. II, we derive the expressions for different terms of the amplitude of reaction (1) in a diagrammatical approach. In Sec. II A, we briefly discuss the main contributions to the reaction amplitude and introduce the notation that we use. In Secs. II B and II C, we give gauge-invariant expressions for the resonance and vector-meson-exchange (VME) contributions to the elementary amplitudes on the nucleon. These results are used in Secs II D and II E to obtain single- and double-scattering amplitudes of reaction (1), respectively. In Sec. III, we present the numerical results. In Sec. III A, we study the influence of the "nonstatic" corrections that are taken into account in the double-scattering amplitude with intermediate η production. In Sec. III B, we discuss our numerical results for the differential cross section (its energy behavior at several values of $\cos\theta$) of reaction (1) with backward π^0 production. The conclusion is presented in Sec. IV.

II. FORMALISM

A. Diagrams and notation

The diagrams for single- and double-scattering amplitudes $M_{(1)}$ and $M_{(2)}$ of reaction (1) are shown in Figs. 1(a) and 1(b), respectively. The notation for the 4-momentum vectors of the initial, intermediate, and final particles are given in this figure. The circles marked by "i" or "j" correspond to the elementary amplitudes of the subreactions on the nucleons, and indices "i" and "j" specify the contributions to the elementary amplitudes considered in the following. In Fig. 1(b), the notation "h" stands for the intermediate meson. Hereafter, we shall consider only diagrams with $h = \pi$ or η.

The elementary photoproduction amplitude $\gamma N \to hN$ is usually constructed as a sum of Born, VME, and resonance terms [4,5,11]. The Born amplitudes correspond to a set of tree diagrams with NNh coupling and all possible couplings with a photon, summed by a contact $\gamma\pi NN$-coupling term. It is known that the total Born amplitude satisfies gauge invariance (see Ref. [4] and references therein). Using Born amplitudes for subprocesses in reaction (1) on the deuteron, one encounters the problem of how to get the total gauge-invariant amplitude. The problem arises from nucleon off-shell effects, and the way to solve it is discussed, for example, in Ref. [8] (see also references therein). However, in our analysis, we shall neglect Born terms in the kinematical region of the reaction under study.

The resonance and VME terms in the photoproduction amplitude are shown graphically in Fig. 2, where VME terms are calculated via ρ and ω exchanges [4,11]. The "meson-meson" $hN \to \pi N$ amplitudes are written through resonance contributions (Fig. 3). The main contribution from an intermediate η meson to the cross section of reaction (1) is expected from the double-scattering diagram in Fig. 1(b) ($h = \eta$), with the $N(1535)$ excitation in both blocks of the diagram attributed to the large partial width of the decay $N(1535) \to \eta N$. Several nucleon resonances [17] are coupled to the πN system. Also, the couplings of $N(1535)$, $N(1440)$, and $N(1520)$ to the ηN system [7,12,13] are often used in the production amplitudes. However, in our qualitative analysis, we shall limit the resonance parts of the elementary amplitudes (Figs. 2 and 3) to the contributions of the $N(1535)$ in the πN and ηN channels and of the $N(1440)$ in the πN channel. We do not include the contribution of the $\Delta(1232)$ isobar since the considered energies are far above the $\Delta(1232)$ region.

Let us write the total amplitude $M_{\gamma d}$ of reaction (1) as

$$M_{\gamma d} = M_{(1)} + M_{(2)}, \qquad M_{(1)} = \sum_i M_i,$$
$$M_{(2)} = \sum_{i,h,j} M_{ihj}, \tag{2}$$

where $h = \pi, \eta$ and index $i = 1, 2, \omega$, and ρ (the same for j) stands for $N(1535)$, $N(1440)$, ω exchange, and ρ exchange for the elementary subprocesses, respectively. Note that the ρ-exchange term in the single-scattering amplitude $M_{(1)}$ is forbidden by isotopic arguments. We shall use standard normalizations for the amplitudes, corresponding to the following expression of the differential cross section for a binary reaction:

$$\frac{d\sigma}{d\Omega_{\text{c.m.}}} = \frac{k}{64\pi^2 s\, q}\overline{|M|^2}. \tag{3}$$

Here, $\overline{|M|^2}$ is the square of the total amplitude, averaged (summed) over the polarizations of the initial (final) particles; s is the square of the total c.m. energy; and q with k are the relative 3-momenta of the initial and final state particles. In the following, we use the notation $\varphi_{1,2}(\chi_{1,2})$ for Pauli spinors (isospinors) for the initial and final nucleons in the elementary reactions or for the nucleons in the deuteron and $\varphi^+\varphi = 1(\chi^+\chi = 1)$; $\check{a} \equiv (\mathbf{a}\boldsymbol{\sigma})$, where $\boldsymbol{a}$ is any 3-vector and $\boldsymbol{\sigma}$ is a 3-vector from the Pauli spin matrices.

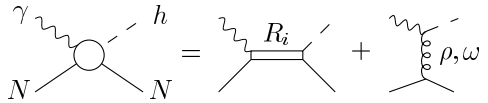

FIG. 2. Diagrams of meson photoproduction on the nucleon (resonance and VME contributions).

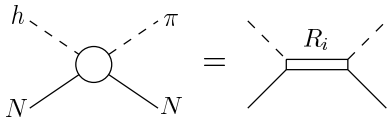

FIG. 3. Diagrams of meson-nucleon binary reactions (resonance contributions).

In Secs. II B and II C, we give gauge-invariant expressions for the elementary amplitudes on the nucleon and notation for coupling constants and other terms that will be used for the total amplitude $M_{\gamma d}$ in Secs. II D and II E.

B. Resonance terms in the amplitudes on the nucleon

To obtain the expressions for resonance contributions to the elementary amplitudes, let us use the effective Lagrangians for the πNR, ηNR, and γNR interactions:

$$\begin{aligned} L_{\pi NR} &= -ig_{\pi NR}\bar{N}\Gamma\boldsymbol{\tau}R\boldsymbol{\pi} + \text{H.c.},\\ L_{\eta NR} &= -ig_{\eta NR}\bar{N}\Gamma R\,\eta + \text{H.c.}, \end{aligned} \tag{4}$$

$$L_{\gamma NR} = \frac{e}{2(m+m_R)}\bar{R}\big(k_R^s + k_R^v\tau_3\big)\Gamma_{\mu\nu}NF^{\mu\nu} + \text{H.c.} \qquad (e^2/4\pi \approx 1/137), \tag{5}$$

$$\Gamma = 1, \qquad \Gamma_{\mu\nu} = \gamma_5\sigma_{\mu\nu} \qquad \text{(odd parity)}, \tag{6}$$

$$\Gamma = \gamma_5, \qquad \Gamma_{\mu\nu} = \sigma_{\mu\nu} \qquad \text{(even parity)} \tag{7}$$

[we use the pseudoscalar couplings in Eq. (4)]. Here, $\sigma_{\mu\nu} = (1)/(2i)(\gamma_\mu\gamma_\nu - \gamma_\nu\gamma_\mu)$; $F^{\mu\nu} = \partial^\nu A^\mu - \partial^\mu A^\nu$; N, $\boldsymbol{\pi}$, η, A^μ, and R are the nucleon, η, π, photon, and resonance-particle (R) fields; m and m_R are the nucleon and resonance masses; and k_R^s and k_R^v correspond to isoscalar and isovector γNR couplings. Operator structures in Eqs. (6) and (7) correspond to odd- $[N(1535), I(J^{PC}) = \frac{1}{2}(\frac{1}{2}^-)]$ and even- $[N(1440), I(J^{PC}) = \frac{1}{2}(\frac{1}{2}^+)]$ parity resonances R.

Hereafter, we use the photon couplings $\hat{g}_{\gamma i}$, g_{si}, and g_{vi}, defined as

$$\hat{g}_{\gamma i} = g_{si} + g_{vi}\tau_3 = \frac{e}{m+m_i}\big(k_R^s + k_R^v\tau_3\big), \tag{8}$$

where $i = 1[N(1535)]$ and $2[N(1440)]$ specifies resonances and their masses m_i.

In the following, we use the nonrelativistic deuteron wave function (DWF) to obtain the amplitudes of reaction (1) (Secs. II D and II E). In this connection, we derive the elementary amplitudes in a nonrelativistic approximation before they are used to obtain the amplitudes on the deuteron, leaving the leading terms only with respect to the relative momenta. The relative accuracy of this approximation near the η-photoproduction threshold ($\sqrt{s} \sim m + m_\eta$) is of the order of $q/2m \sim 0.2$–0.3 (where q is the photon relative momentum). Let us introduce some useful notation for the resonance amplitude A_{aib} of the reaction $aN \to R_i \to bN$, writing it as

$$A_{aib} = \chi_2^+\hat{T}\chi_1\,\varphi_2^+\hat{S}\varphi_1, \qquad \hat{T} = \hat{T}_{aib}, \qquad \hat{S} = \hat{S}_{aib}, \tag{9}$$

where $\hat{S}$ and $\hat{T}$ are spin and isospin operators. Let us first consider the spin operators, $\hat{S}_{\gamma ih}$, of the photoproduction amplitudes. In our approximation, they have the following structures:

$$\hat{S}_{\gamma 1h} \sim (q_0\,\check{e} - e_0\,\check{q}), \qquad \hat{S}_{\gamma 2h} \sim \check{k}(\check{q}\,\check{e} - q_0\,e_0),$$

where $\check{e} = (\boldsymbol{\sigma e})$, $\check{q} = (\boldsymbol{\sigma q})$, and $\check{k} = (\boldsymbol{\sigma k})$; $\boldsymbol{k}$ ($\boldsymbol{q}$) is the c.m. 3-momentum of the final meson (initial photon); q_0 and $e = (e_0, \boldsymbol{e})$ are the c.m. energy and polarization 4-vector of the photon. Note that gauge invariance, guaranteed by the Lagrangian $L_{\gamma NR}$ (5), is obviously valid for the operators $\hat{S}_{\gamma 1h}$ and $\hat{S}_{\gamma 2h}$. Hereafter, we shall fix the photon 4-vector by the gauge condition $e_0 = (\boldsymbol{eq}) = 0$. Finally, we obtain the following expessions for the resonance amplitudes A_{aib} in terms of the operators $\hat{T}_{aib}$ and $\hat{S}_{aib}$ (9):

$$\begin{aligned} \hat{T}_{\gamma i\pi} &= (\boldsymbol{\pi\tau})\hat{g}_{\gamma i}, & \hat{T}_{\gamma i\eta} &= \hat{g}_{\gamma i},\\ \hat{T}_{\pi_1 i\pi_2} &= (\boldsymbol{\pi}_2\boldsymbol{\tau})(\boldsymbol{\pi}_1\boldsymbol{\tau}), & \hat{T}_{\eta i\pi} &= (\boldsymbol{\pi\tau}) \quad (i = 1, 2),\\ \hat{S}_{\gamma 1h} &= iC_{\gamma 1h}F_{1h}\check{e}, & \hat{S}_{\gamma 2h} &= iC_{\gamma 2h}F_{2h}\check{k}\,\check{q}\,\check{e},\\ \hat{S}_{h1\pi} &= iC_{h1\pi}F_{1h}F_{1\pi}\mathbf{I} & & (h = \pi, \eta),\\ C_{\gamma 1h} &= g_{1h}BW_1 2mq_0, & C_{\gamma 2h} &= g_{2h}BW_2,\\ C_{h1\pi} &= ig_{1h}g_{1\pi}BW_1 2m, & \hat{S}_{h2\pi} &= iC_{h2\pi}F_{2h}F_{2\pi}\check{k}\check{q},\\ C_{h2\pi} &= \frac{i}{2m}g_{2h}g_{2\pi}BW_1, & BW_i &= \frac{2m_i}{s - m_i^2 + i\sqrt{s}\Gamma_i(s)}, \end{aligned} \tag{10}$$

where, in addition to the previous notation, $\boldsymbol{q}$ is the c.m. 3-momentum of the initial photon or meson; $BW_i, \Gamma_i(s)$, and g_{ih} are the Breit-Wigner propagator, total width, and coupling constant to the hN channel for the ith resonance, respectively; $\mathbf{I}$ is the unit 2×2 matrix; and F_{ih} are the form factors of the strong decays $R_i \to hN$. Here, we use the form factor only for the p-wave $N(1440)N\pi$ vertex ($F_{ih} \equiv 1$ for other vertices) to compensate for its energy growing in the region far away from the πN threshold. We take the function $F_{2\pi} = F$ in a monopole parametrization [see Eqs. (11)], which is convenient for analytical calculations of the integrals in Sec. II D. The widths Γ_i, coupling constants g_{ih}, and relative 3-momenta $q_h (h = \pi, \eta)$ for the decays $N(1535) \to \pi N, \eta N$ and $N(1440) \to \pi N$ are connected by the relations

$$\begin{aligned} \Gamma_1(s) &= \Gamma_{1\pi}(s) + \Gamma_{1\eta}(s), & \Gamma_{1\pi} &= 3g_{1\pi}^2\frac{(E+m)q_\pi}{4\pi\sqrt{s}},\\ \Gamma_{1\eta} &= g_{1\eta}^2\frac{(E+m)q_\eta}{4\pi\sqrt{s}}, & \Gamma_{2\pi} &= 3g_{2\pi}^2\frac{(E-m)q_\pi}{4\pi\sqrt{s}}F^2(q_\pi),\\ F(q_\pi) &= \frac{\Lambda_0^2}{\Lambda^2 + q_\pi^2}, & \Lambda_0^2 &= \Lambda^2 + q_{0\pi}^2, \end{aligned} \tag{11}$$

where $E + m \approx 2m$, $E - m \approx q_\pi^2/(2m)$ (where E is nucleon total energy), and $q_{0\pi}$ is the relative momentum in the decay $N(1440) \to \pi N$ at resonance mass.

The photon couplings $\hat{g}_{\gamma i}$ can be expressed through helicity amplitudes $A_{1/2}^p$ and $A_{1/2}^n$ [11] of the decays $R_i \to p\gamma$ and $R_i \to n\gamma$, respectively. We can relate the radiative widths to the amplitudes $A_{1/2}^{p,n}$ (for spin-1/2 resonances) as well as to the

constants $g^{p,n}_{\gamma i} = g_{si} \pm g_{vi}$; that is,

$$\Gamma(R_i \to p\gamma, n\gamma) = \frac{k_\gamma^2 m}{\pi m_i}\left|A^{p,n}_{1/2}\right|^2 = \left(g^{p,n}_{\gamma i}\right)^2 \frac{k_\gamma^3}{\pi}, \qquad (12)$$

where k_γ is the relative photon 3-momentum in the decay. Then, we obtain

$$\left|A^{p,n}_{1/2}\right|^2 = \left(g^{p,n}_{\gamma i}\right)^2 \frac{m_i}{m} k_\gamma, \qquad 2g_{vi} = \left(A^p_{1/2} - A^n_{1/2}\right)\sqrt{\frac{m}{m_i k_\gamma}}. \qquad (13)$$

Note that only the isovector constants g_{vi} (not g_{si}) are needed to derive the amplitude for reaction (1) on the deuteron. The helicity amplitudes are usually extracted from the photoproduction experiments, and the values $A^{p,n}_{1/2}$ for $N(1535)$, $N(1440)$, and other nucleon resonances can be found, for example, in Refs. [5,18].

C. Vector-meson exchange terms

To derive ω- and ρ-exchange amplitudes of the photoreactions on the nucleon, we use the effective Lagrangians L_{VNN} and $L_{\rm em}$ of the $VNN(V = \omega, \rho)$ and $Vh\gamma(h = \pi, \eta)$ interaction, taken in forms used in Refs. [4,11] as

$$L_{VNN} = -g_{VNN}\bar{N}\left[\left(\gamma_\mu + \frac{\beta_V}{2m}\sigma_{\mu\nu}\partial^\nu\right)(\omega^\mu + \boldsymbol{\tau}\boldsymbol{\rho}^\mu)\right]N, \qquad (14)$$

$$L_{\rm em} = \epsilon_{\mu\nu\lambda\sigma}(\partial^\mu e^\nu)\left[\frac{G_{V\pi\gamma}}{m_\pi}(\partial^\lambda \pi_i)\left(\delta_{i3}\omega^\sigma + \rho_i^\sigma\right) + \frac{G_{V\eta\gamma}}{m_\eta}(\partial^\lambda\eta)\delta_{i3}\rho_i^\sigma\right] \qquad (15)$$

($\epsilon_{1230} = 1, \epsilon_{123} = 1$), where $\mu, \nu, \lambda, \sigma$ and i, j are Lorentz and isotopic indices, respectively, and π, η, ρ, and ω stand for π, η, ρ, and ω mesons. The coupling constants $G_{Vh\gamma}(h = \pi, \eta)$ in Eq. (15) can be expressed through the radiative widths $\Gamma_{V\to h\gamma}$ by the following relation:

$$\Gamma_{V\to h\gamma} = \frac{G^2_{Vh\gamma} q^3_{h\gamma}}{12\pi m_h^2} = \frac{G^2_{Vh\gamma}}{12\pi m_h^2}\frac{m_V^3}{8}\left(1 - \frac{m_h^2}{m_V^2}\right)^3. \qquad (16)$$

Using Eqs. (14) and (15), one can write the VME amplitudes of the reactions $\gamma N \to hN$ as $A_{\gamma Vh} = \chi_2^+ \hat{T}\chi_1 \bar{u}_2 \hat{M}_{\gamma Vh} u_1$, where $u_{1,2}$ are nucleon Dirac spinors ($\bar{u}_{1,2}u_{1,2} = 2m$), and

$$\hat{M}_{\gamma Vh} = \frac{G_{Vh\gamma}}{m_h}\frac{g_{VNN}}{\left(r^2 - m_V^2\right)}\epsilon_{\mu\nu\lambda\sigma} q^\mu e^\nu k^\lambda \times\left[-(1+\beta_V)\gamma^\sigma + \frac{\beta_V}{m}p_1^\sigma\right], \qquad (17)$$

where q^μ and e^ν are the 4-momentum and polarization of the photon, k^λ and p^σ are 4-momenta of the final meson h and the initial nucleon, and $r^2 = (q-k)^2$ is the 4-momentum transfer to the nucleon squared. $\hat{T} = \hat{T}_{\gamma Vh}$ is the isospin operator:

$$\hat{T}_{\gamma\rho\pi} = (\boldsymbol{\pi}\boldsymbol{\tau}), \qquad \hat{T}_{\gamma\omega\pi} = (\boldsymbol{n}_3\boldsymbol{\pi})\mathbf{I}, \qquad \hat{T}_{\gamma\rho\eta} = \tau_3, \qquad (18)$$

where $\boldsymbol{n}_3 = (0, 0, 1)$ is the unit vector in isotopic space. Using the notation (9) for the amplitude $A_{\gamma Vh}$ (i.e., $\bar{u}_2\hat{M}_{\gamma Vh}u_1 = \varphi_2^+\hat{S}_{\gamma Vh}\varphi_1$) and the gauge invariance condition $e_0 = (\boldsymbol{eq}) = 0$, in the nonrelativistic approximation, we have

$$\hat{S}_{\gamma Vh} = iC_{\gamma Vh}\,\mathrm{Tr}\{\check{k}\check{q}\check{e}\}\mathbf{I}, \qquad C_{\gamma Vh} = \frac{m}{m_h}\frac{G_{Vh\gamma}g_{VNN}}{\left(r^2 - m_V^2\right)},$$
$$\mathrm{Tr}\{\check{k}\check{q}\check{e}\} = 2i(\boldsymbol{k}\cdot[\boldsymbol{q}\times\boldsymbol{e}]). \qquad (19)$$

(Here, the expression for the trace $\mathrm{Tr}\{\check{k}\check{q}\check{e}\}$ is used for convenience in Sec. II D.) The amplitudes (19) in our approximation do not contain the constants β_V from Eq. (14). The gauge invariance of the amplitude (17) is obvious and is also satisfied in the expression (19) for $\hat{S}_{\gamma Vh}$ owing to the gauge-invariant factor $\mathrm{Tr}\{\check{k}\check{q}\check{e}\}$.

Note that the $\rho\pi\gamma$ vertex in the Lagrangian (15) corresponds to isoscalar photon coupling, whereas only isovector photon coupling can contribute to the amplitude of reaction (1). Generally, the isotopic $\rho\pi\gamma$ vertex has the structure $g_1(\boldsymbol{\pi}\boldsymbol{\rho}) + g_2\pi_3\rho_3 + g_3(\boldsymbol{n}_3[\boldsymbol{\pi}\times\boldsymbol{\rho}])$, where g_3 is an isovector coupling constant. Then for radiative ρ decays, we have $\Gamma_{\rho^0\to\pi^0\gamma} \sim (g_1+g_2)^2$ and $\Gamma_{\rho^\pm\to\pi^\pm\gamma} \sim g_1^2 + g_3^2$. From the PDG [17], $\Gamma_{\rho^0\to\pi^0\gamma}/\Gamma_{\rho^\pm\to\pi^\pm\gamma} \sim 1.7$–$1.8$, that is, $(g_1+g_2)^2 > g_1^2 + g_3^2$. Since isoscalar $\rho\pi\gamma$ coupling ($g_2 = g_3 = 0$) is successfully used in the ρ-exchange amplitude of the reaction $\gamma N \to \pi N$, we may suppose that $g_{2,3} \ll g_1$. In addition, let us compare ω- and ρ-exchange amplitudes $M_{\gamma\omega\pi}$ and $M_{\gamma\rho\pi}$ of the reaction $\gamma N \to \pi^0 N$. Using coupling constants from [4] ($g_1 \equiv G_{\rho\pi\gamma}$), we obtain $M_{\gamma\omega\pi}/M_{\gamma\rho\pi} \sim G_{\omega\pi\gamma}g_{\omega NN}/G_{\rho\pi\gamma}g_{\rho NN} \sim 10$. Based on that, we neglect the ρ-exchange amplitude with intermediate pion production in reaction (1) in comparison with the ω-exchange amplitude.

D. Single-scattering amplitude of the reaction $\gamma d \to \pi^0 d$

Let us write the amplitude A of the process $\gamma N \to \pi^0 N$ in the form (9), where $\hat{S}$ and $\hat{T}$ are the spin and isospin parts of the transition operator. Then, a single-scattering amplitude $M_{(1)}$ for reaction (1) reads

$$M_{(1)} = 2\,\mathrm{Tr}\{\hat{T}\}\int\frac{d^3\mathbf{p}}{(2\pi)^3}\,\mathrm{Tr}\left\{\hat{\Psi}_2^+\hat{S}\hat{\Psi}_1\right\}, \quad \hat{\Psi}_{1,2} = \hat{\Psi}(\boldsymbol{\epsilon}_{1,2}, \boldsymbol{q}_{1,2}). \qquad (20)$$

Here, the intermediate nucleon with 3-momentum $\boldsymbol{p}$ [see Fig. 1(a)] is on-shell; $\boldsymbol{q}_{1,2} = \boldsymbol{p} - \frac{1}{2}\boldsymbol{P}_{1,2}$; $\boldsymbol{\epsilon}_{1,2}$ are 3-vectors of polarization for initial and final deuterons; and $\hat{\Psi}(\boldsymbol{\epsilon}, \boldsymbol{q})$ is a matrix expression in the DWF Ψ, which has the form

$$\Psi = \varphi_2^+\hat{\Psi}\sigma_2\varphi_1^*\chi_2^+\frac{\tau_2}{\sqrt{2}}\chi_1^*,$$
$$\hat{\Psi} = \hat{\Psi}(\boldsymbol{\epsilon}, \boldsymbol{q}) = \frac{u(q)}{\sqrt{2}}\check{\epsilon} - \frac{w(q)}{2}\left(\frac{3(\boldsymbol{q}\boldsymbol{\epsilon})}{q^2}\check{q} - \check{\epsilon}\right), \qquad (21)$$

where $\boldsymbol{q}$ is the relative 3-momentum of nucleons, $u(q)$ and $w(q)$ are the s- and d-wave parts of the DWF, respectively, normalized as $\int d^3\boldsymbol{q}[u^2(q) + w^2(q)] = (2\pi)^3$ (we follow the diagrammatical technique of Ref. [19], and some comments will be given in Sec. II E).

Then, using Eqs. (9), (10), (18), and (19) for the $\gamma N \to \pi^0 N$ amplitudes, we obtain

$$M_{(1)} = M_1 + M_2 + M_\omega, \qquad M_i = x_i \int \frac{d^3\mathbf{p}}{(2\pi)^3} \mathrm{Tr}\{\hat\Psi_2^+ \hat O_i \hat\Psi_1\} \quad (i = 1, 2, \omega),$$
$$\hat O_1 = \check e, \qquad \hat O_2 = \check k \check q \check e, \qquad \hat O_\omega = \mathrm{Tr}\{\check k \check q \check e\}\mathbf{I},$$
$$x_1 = 4ig_{v1}C_{\gamma 1\pi}, \quad x_2 = 4ig_{v2}C_{\gamma 2\pi}F(k), \quad x_\omega = 4iC_{\gamma\omega\pi}. \tag{22}$$

Hereafter, q_0, $\boldsymbol{q}$, and $\boldsymbol{k}$ are the c.m. photon energy and the c.m. 3-momenta of the initial photon and final pion, respectively. The values $x_{1,2}$, factored out of the integrals in Eq. (22), depend on the effective mass $m_{\pi N} = \sqrt{s}$ in the subprocess $\gamma N \to \pi N$, and we calculate the value $m_{\pi N}$ using the 3-momentum $\boldsymbol{p} = \frac{1}{4}(\boldsymbol{P}_1 + \boldsymbol{P}_2)$ of the intermediate nucleon in Fig. 1(a). Expressing the DWF given by Eq. (21) for $\hat\Psi$ in the $\boldsymbol{r}$-representation, where

$$\hat\Psi(\boldsymbol{\epsilon}, \boldsymbol{q}) = \int \frac{d^3\mathbf{r}}{4\pi} e^{-i\boldsymbol{q}\boldsymbol{r}} \hat\Phi(\boldsymbol{\epsilon}, \boldsymbol{r}),$$
$$\hat\Phi(\boldsymbol{\epsilon}, \boldsymbol{r}) = \frac{u(r)}{r\sqrt{2}}\check\epsilon - \frac{w(r)}{2r}\left(\frac{3(\boldsymbol{r}\boldsymbol{\epsilon})}{r^2}\check r - \check\epsilon\right), \tag{23}$$

we obtain the amplitudes M_i (22) in the form

$$M_i = x_i \int \frac{d^3\boldsymbol{r}}{(4\pi)^2} e^{i\boldsymbol{\Delta}\boldsymbol{r}} \mathrm{Tr}\{\hat\Phi_2^+ \hat O_i \hat\Phi_1\},$$
$$\hat\Phi_{1,2} = \hat\Phi(\boldsymbol{\epsilon}, \boldsymbol{r}), \qquad \boldsymbol{\Delta} = \frac{1}{2}(\boldsymbol{k} - \boldsymbol{q}). \tag{24}$$

To evaluate the amplitudes M_i, let us introduce the integrals

$$\int \frac{d^3\boldsymbol{r}}{(4\pi)^2} e^{i\boldsymbol{\Delta}\boldsymbol{r}} f_1^2(r) = A_1,$$
$$\int \frac{d^3\boldsymbol{r}}{(4\pi)^2} e^{i\boldsymbol{\Delta}\boldsymbol{r}} f_{1,2}(r) f_2(r) \frac{r_i r_j}{r^2} = n_i n_j B_{1,2} + \delta_{ij} C_{1,2}, \tag{25}$$

where

$$f_1(r) = \frac{u(r)}{r\sqrt{2}} + \frac{w(r)}{2r}, \qquad f_2(r) = \frac{3w(r)}{2r},$$
$$\mathbf{n} = \frac{\mathbf{del}}{\Delta} \quad (|\mathbf{n}| = 1). \tag{26}$$

From Eqs. (22)–(26), we obtain the amplitudes M_i ($i = 1, 2, \omega$) in the form

$$M_1 = x_1(A_1 - 2C_1)\,\mathrm{Tr}\{\check\epsilon_2^* \check e \check\epsilon_1\} + x_1 B_1\,\mathrm{Tr}\{\check V \check e \check n\},$$
$$M_2 = x_2(A_1 - 2C_1)\,\mathrm{Tr}\{\check\epsilon_2^* \check k \check q \check e \check\epsilon_1\} + x_2 B_1\,\mathrm{Tr}\{\check V \check k \check q \check e \check n\}$$
$$+ x_2[C_2(\boldsymbol{\epsilon}_1\boldsymbol{\epsilon}_2^*) + (B_2 - 2B_1)(\boldsymbol{n}\boldsymbol{\epsilon}_1)(\boldsymbol{n}\boldsymbol{\epsilon}_2^*)]\,\mathrm{Tr}\{\check k \check q \check e\},$$
$$M_\omega = 2x_\omega[(A_1 - 2C_1 + C_2)(\boldsymbol{\epsilon}_1\boldsymbol{\epsilon}_2^*)$$
$$+ (B_2 - 2B_1)(\boldsymbol{n}\boldsymbol{\epsilon}_1)(\boldsymbol{n}\boldsymbol{\epsilon}_2^*)]\,\mathrm{Tr}\{\check k \check q \check e\}, \tag{27}$$

where $\check V = (\boldsymbol{n}\boldsymbol{\epsilon}_2^*)\check\epsilon_1 - (\boldsymbol{n}\boldsymbol{\epsilon}_1)\check\epsilon_2^*$ ($\check\epsilon_2^* = \boldsymbol{\epsilon}_2^*\boldsymbol{\sigma}$). Neglecting the d-wave component of the DWF [i.e., setting $w(r) = 0$ in Eq. (26)], one obtains $B_{1,2} = C_{1,2} = 0$, which simplifies Eqs. (27). However, in a single-scattering amplitude, the momentum is transferred to one nucleon, and at large angles of the outgoing π^0, the relative momenta $q_{1,2}$ of the nucleons become large and the d-wave part of the DWF should be important. We use a parametrization of the DWF employing the Bonn potential [20] (full model) and the corresponding analytical expressions for A_1, $B_{1,2}$, and $C_{1,2}$, used in Eqs. (27), are given in the extended version of the present paper [21].

E. Double-scattering amplitude of the reaction $\gamma d \to \pi^0 d$

Let $\hat S_1(\hat S_2)$ and $\hat T_1(\hat T_2)$ be spin and isospin operators in the amplitude (9) of the subprocess $\gamma N \to hN (hN \to \pi^0 N)$ in the diagram of Fig. 1(b). Then, the double-scattering amplitude $M_{(2)}$ has the form

$$M_{(2)} = -\frac{1}{m}\mathrm{Tr}\{\hat T_1 \hat T_2^c\} \int \frac{d^3\boldsymbol{p}_2}{(2\pi)^3}\frac{d^3\boldsymbol{p}_1'}{(2\pi)^3}\mathrm{Tr}\{\hat\Psi_2^+ \hat S_1 \hat\Psi_1 \hat S_2^c\} G_h(s), \tag{28}$$

where integration over the energies of intermediate nucleons with 3-momenta $\boldsymbol{p}_1'$ and $\boldsymbol{p}_2$ [see Fig. 1(b)] has already been done, giving the result (28) with those nucleons taken on the mass shell. Here, $G_h(s)$ is the propagator of the intermediate meson h with 3-momentum $\boldsymbol{s}$ and $\hat T_2^c = \tau_2 \hat T^T \tau_2$ and $\hat S_2^c = \sigma_2 \hat S^T \sigma_2$ [22], where index "T" stands for transposition operator.

Inserting $\hat T$ and $\hat S$ from Eqs. (10), (18), and (19), we obtain the contributions M_{ihj} to $M_{(2)}$ in the form

$$M_{ihj} = -y_{ihj} \int \frac{d^3\boldsymbol{p}_2}{(2\pi)^3}\frac{d^3\boldsymbol{p}_1'}{(2\pi)^3}\mathrm{Tr}\{\hat O_{ihj}\} G_h(s),$$
$$y_{ih1} = \frac{2g_{vi}}{m} C_{\gamma ih} C_{h1\pi}, \qquad \hat O_{1h1} = \hat\Psi_2^+ \check e \hat\Psi_1,$$
$$\hat O_{2\pi 1} = \hat\Psi_2^+ \check s \check q \check e \hat\Psi_1 \check s \check k F(s), \qquad y_{ih2} = \frac{2g_{vi}}{m} C_{\gamma ih} C_{h2\pi} F(k),$$
$$\hat O_{1\pi 2} = \hat\Psi_2^+ \check e \hat\Psi_1 \check s \check k F(s), \qquad \hat O_{2\pi 2} = \hat\Psi_2^+ \check s \check q \check e \hat\Psi_1 \check s \check k F^2(s), \tag{29}$$

where $F(s)$ is a form factor in the $N(1440)N\pi$ vertex [see Eq. (11)]. For simplicity in this paper, we do not take into account VME contributions in the double-scattering amplitudes.

For the double-scattering amplitude due to the DWF, the main contribution to the integral $\int d^3\boldsymbol{p}_2 d^3\boldsymbol{p}_1'$ comes from the regions $\boldsymbol{p}_{1,2} \sim \frac{1}{2}\boldsymbol{P}_1$ and $\boldsymbol{p}_{1,2}' \sim \frac{1}{2}\boldsymbol{P}_2$ with small relative momenta $q_{1,2} \sim 0$. To simplify the calculations, we neglect the d-wave components of the DWF in the amplitudes M_{ihj}. The factors y_{ihj} in Eqs. (29) are calculated at

$$\boldsymbol{p}_1 = \boldsymbol{p}_2 = \tfrac{1}{2}\boldsymbol{P}_1, \qquad \boldsymbol{p}_1' = \boldsymbol{p}_2' = \tfrac{1}{2}\boldsymbol{P}_2. \tag{30}$$

The meson propagator $G_h(s) = (s^2 - m_h^2 + i0)^{-1}$ in Eq. (29) can be written as

$$G_h(s) = -\left[\boldsymbol{s}^2 + \frac{Q_0}{m}\left(\boldsymbol{p}_1'^2 + \boldsymbol{p}_2^2\right) + a_h^2 - i0\right]^{-1},$$
$$Q_0 = q_0 + T_{d1} - \varepsilon_d, \qquad a_h^2 = m_h^2 - Q_0^2, \tag{31}$$

where, T_{d1} is the kinetic c.m. energy of the initial deuteron, $\boldsymbol{s} = -\boldsymbol{p}_1' - \boldsymbol{p}_2$, and Q_0 is the excess energy in the process $\gamma d \to pnh$. The term $(Q_0/m)(\boldsymbol{p}_1'^2 + \boldsymbol{p}_2^2)$ in Eq. (31) takes into account the kinetic energies of the intermediate nucleons.

In this section, we neglect this term; that is, we use a "static" approximation. However, to study the energy dependence of the differential cross section of η production ($Q_0 \sim m_\eta$) in the threshold region, we shall restore this term in the amplitude with the intermediate η meson in Sec. III A.

Note that the spin structure of the elementary amplitudes [$N(1440)$ contribution] includes the dependence on the 3-momentum $\boldsymbol{s}$ of the intermediate meson h in Fig. 1(b). This dependence is taken into account in the double-scattering amplitudes (29). Here, let us mention that similar calculations were presented long ago in Ref. [23] for elastic πd scattering in the $\Delta(1232)$ region and a two-loop integral was calculated with angular dependence of the πN amplitude taken into account. In the following, we give some details of our calculations of the amplitudes M_{ihj} (29).

In the "static" approximation, $G_h = -(\boldsymbol{s}^2 + a_h^2 - i0)^{-1}$. The $\boldsymbol{r}$-representation is convenient for calculating the double-scattering amplitudes. Let us introduce the Fourier transformations for $\boldsymbol{s}$-dependent parts of the integrands (29):

$$\begin{aligned}
\frac{1}{\mathbf{s^2} + \mathbf{a_h^2} - \mathbf{i0}} &= \int \frac{d^3\mathbf{r}}{4\pi} e^{i\boldsymbol{s}\boldsymbol{r}} h_{11}(r), \\
\frac{\mathbf{sF(s)}}{\mathbf{s^2} + \mathbf{a_h^2} - \mathbf{i0}} &= \int \frac{d^3\mathbf{r}}{4\pi} e^{i\boldsymbol{s}\boldsymbol{r}} \boldsymbol{r} h_{12}(r), \\
\frac{s_i s_j}{\mathbf{s^2} + \mathbf{a_h^2} - \mathbf{i0}} F^2(s) &= \int \frac{d^3\mathbf{r}}{4\pi} e^{i\boldsymbol{s}\boldsymbol{r}} [r_i r_j h_1(r) + \delta_{ij} r^2 h_2(r)].
\end{aligned} \tag{32}$$

Let us also define the integrals

$$\begin{aligned}
\int f^2(r) h_{11}(r) &= A_{11}, \qquad \int f^2(r) h_{12}(r) \boldsymbol{r} = \boldsymbol{m} A_{12}, \\
\int f^2(r) h_1(r) r_i r_j &= m_i m_j A_{221} + \delta_{ij} A_{222}, \\
\int f^2(r) r^2 h_2(r) &= A_{223},
\end{aligned} \tag{33}$$

where $f(r) = u(r)/(r\sqrt{2})$, and $u(r)$ is the s-wave part of the DWF. For the integrals in Eqs. (33), we use a shorthand notation

$$\int \ldots \equiv \int \frac{d^3\mathbf{r}}{(4\pi)^3} e^{i\boldsymbol{Q}\boldsymbol{r}} \ldots, \qquad \boldsymbol{Q} = \frac{1}{2}(k + \boldsymbol{q}), \qquad \boldsymbol{m} = \frac{\mathbf{Q}}{Q}. \tag{34}$$

The functions $h_{11,12,1,2}(r)$ and the expressions for A_{11}, A_{12}, A_{221}, and A_{222} are given in Ref. [21]. Rewriting integrals (29) in the $\boldsymbol{r}$ representation using Eqs. (23), (32), and (33), we obtain the following expressions for amplitudes M_{ihj}:

$$\begin{aligned}
M_{1h1} &= y_{1h1} A_{11} \,\mathrm{Tr}\{\check{\epsilon}_2^* \check{e} \check{\epsilon}_1\} \quad (h = \pi, \eta), \\
M_{1\pi 2} &= y_{1\pi 2} A_{12} \,\mathrm{Tr}\{\check{\epsilon}_2^* \check{e} \check{\epsilon}_1 \check{m} \check{k}\}, \\
M_{2\pi 1} &= y_{2\pi 1} A_{12} \,\mathrm{Tr}\{\check{\epsilon}_2^* \check{m} \check{q} \check{e} \check{\epsilon}_1\}, \\
M_{2\pi 2} &= y_{2\pi 2} [A_{221} \,\mathrm{Tr}\{\check{\epsilon}_2^* \check{m} \check{q} \check{e} \check{\epsilon}_1 \check{m} \check{k}\} \\
&\quad + (A_{222} + A_{223}) \,\mathrm{Tr}\{\check{\epsilon}_2^* \boldsymbol{\sigma} \check{q} \check{e} \check{\epsilon}_1 \boldsymbol{\sigma} \check{k}\}].
\end{aligned} \tag{35}$$

By summing the amplitudes from Eqs. (22) and (35), we obtain the total amplitude $M_{\gamma d}$ (2). Note that the gauge invariance of this amplitude comes from the Lagrangians (5) and (15) and that invariance is not violated by the nucleon off-shell effects in the deuteron. The square $\overline{|M_{\gamma d}|^2}$ of the total amplitude, averaged (summed) over initial (final) polarizations, is rather cumbersome, and we do not write it here.

III. NUMERICAL RESULTS

A. Nucleon kinetic energy terms

Before we consider the differential cross section of reaction (1), let us discuss the threshold effect of intermediate η production in the double-scattering amplitude. The contributions of the intermediate η meson to the reaction amplitude comes from the terms $M_{1\eta 1}$ and $M_{\rho\eta 1}$ (35), which contain the integral A_{11}. We shall recalculate A_{11} in a "nonstatic" case using the η propagator (31) with nucleon kinetic energy (NKE) terms $(Q_0/m)(\boldsymbol{p}_1'^2 + \boldsymbol{p}_2^2)$ taken into account, and compare it with the result of the "static" approximation, used in Eqs. (32) and (33).

To simplify the calculation of A_{11} for the "nonstatic" case, let us replace the Bonn DWF by the effective Gaussian s-wave function $\psi(r) = B\exp(-br^2)$. To fix the slope parameter b, let us note that for reaction (1) at the η threshold with backward outgoing π^0, we have $a_h^2 = 0\,(h = \eta)$ in Eq. (31) and $\boldsymbol{Q} \approx 0$ in Eqs. (33). However, we have $A_{11}(a_h^2 = Q = 0) \sim \langle 1/r \rangle_d$ from Eqs. (33). We fix the value b from the mean value $\langle 1/r \rangle_d$ corresponding to the s-wave part of the Bonn DWF. The expression for A_{11} with the Gaussian DWF is given in Ref. [21].

Figure 4 shows $\mathrm{Re}\,A_{11}$ and $\mathrm{Im}\,A_{11}$, calculated in the "static" approximation, as a function of the photon laboratory energy E_γ for one of the values of $z = \cos\theta$, where θ is the c.m. scattering angle of the outgoing π^0 meson. Here, one can see that the results obtained with Bonn (solid curves) and Gaussian (dashed curves) s DWF's are quite close to each other (a characteristic valid in the wide region of z for which we obtain results in this paper). The function $\mathrm{Re}\,A_{11}$ peaks at $E_\gamma = E_{\mathrm{th}} \approx 630$ MeV, where E_{th} is the photon threshold energy for the reaction $\gamma d \to \eta pn$, and $\mathrm{Im}\,A_{11} = 0$ at $E_\gamma < E_{\mathrm{th}}$. Note that the left (right) derivative $d(\mathrm{Re}\,A_{11})/dE_\gamma \to +\infty\,[d(\mathrm{Im}\,A_{11})/dE_\gamma \to +\infty]$ at $E_\gamma \to E_{\mathrm{th}}$. These properties come from the "static" approximation used in Eqs. (32). In the η-threshold region, the function $\mathrm{Im}\,A_{11}$ should depend on E_γ as a 3-particle $NN\eta$ phase space, that is, $\sim Q_0^{3/2}$, where Q_0 is the excess energy given in Eqs. (31) and $Q_0 \approx E_\gamma - E_{\mathrm{th}}$. In fact, when NKE terms $(Q_0/m)(\boldsymbol{p}_1'^2 + \boldsymbol{p}_2^2)$ in the η propagator (31) are neglected, then $\mathrm{Im}\,A_{11}$ behaves as a 2-particle phase space, that is, $\sim Q_0^{1/2}$.

In Fig. 5, we compare $\mathrm{Re}\,A_{11}$, $\mathrm{Im}\,A_{11}$, and $|A_{11}|^2$ calculated with the Gaussian DWF in "static" (dashed curves) and "nonstatic" (solid curves) cases. Results are shown for two z values, -0.55 [Figs. 5(a), 5(c), and 5(e)] and -0.85 [Figs. 5(b), 5(d), and 5(f)]. In the "nonstatic" case, $\mathrm{Im}\,A_{11} \sim Q^{3/2}$ in the small region close to the η threshold and then because of the DWF $\mathrm{Im}\,A_{11}$ begins to decrease where E_γ increases. The energy dependence of $|A_{11}|^2$ clearly demonstrates the

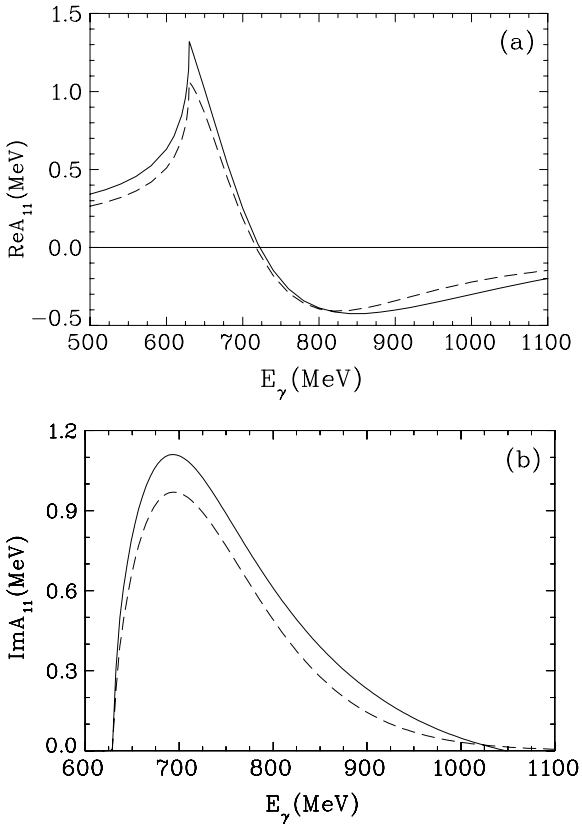

FIG. 4. (a) [(b)] Real [image] parts of the loop integral A_{11} of the double-scattering diagram [Fig. 1(b)] in the "static" approximation with an intermediate η meson in the reaction (1). The results are given for the values $z = \cos\theta = -0.55$. Solid (dashed) curves correspond to the results with the Bonn (Gaussian) s DWF.

η-threshold effect from the loop diagram [Fig. 1(b)] in the energy behavior of the differential cross section of reaction (1) when all kinematical factors from subreactions on the nucleons are neglected. Figures 5(e) and 5(f) show that when NKE terms are included then $|A_{11}|^2$ turns out to be a much smoother function instead of exhibiting the sharp peaking in the "static" approximation case.

Finally, for the differential cross sections in Sec. III B, all double-scattering amplitudes with an intermediate pion are calculated in a "static" approximation using the Bonn DWF [20] and the expressions for the integrals $A_{11,12,221,222,223}$ are defined by Eqs. (33). For the amplitude with an intermediate η meson, we use A_{11} with NKE terms taken into account as described in this section.

B. Differential cross section of the reaction $\gamma d \to \pi^0 d$

The amplitude of reaction (1) as expressed by Eqs. (27) and (35) depends on a number of parameters. In Table I, we list sets of helicity amplitudes $A^{p,n}_{1/2}$ for photon couplings to spin-$\frac{1}{2}$ resonances [see Eqs. (13)] used in our amplitudes.

We use the values $A^{p,n}_{1/2}$ from column [24]-1 (1st variant from Ref. [24]), which are approximately the mean values among those given in Table I.

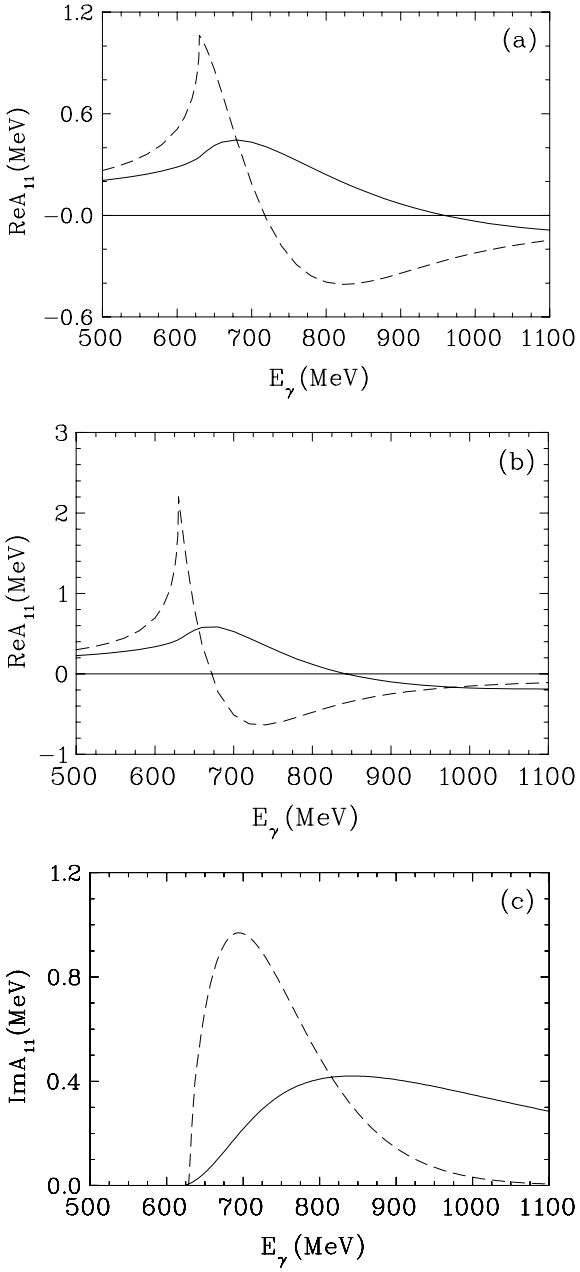

FIG. 5. (a) and (b) Results for ReA_{11}; (c) and (d) results for Im A_{11}; and (e) and (f) results for $|A_{11}|^2$ at $z = -0.55$ [(a), (c), and (e)] and $z = -0.85$ [(b), (d), and (f)] with the Gaussian s DWF. Solid (dashed) curves correspond to the "nonstatic" ("static") case.

For the partial (Γ_{ih}) and total (Γ_i) widths (11) of $N(1535)$ and $N(1440)$ at nominal masses ($\sqrt{s} = m_{1,2}$), we use the values

$$\begin{aligned} \Gamma_{1\pi} &= \Gamma_{1\eta} = 0.5\Gamma_1, & \Gamma_{2\pi} &= 0.65\Gamma_2, \\ \Gamma_1 &= 150\ \text{MeV}, & \Gamma_2 &= 350\ \text{MeV} \end{aligned} \tag{36}$$

and take $\Lambda = 1$ GeV in the form factor F (11) of the hadronic $N(1440)$ decay.

The coupling constant $G_{\omega\pi\gamma}$ is obtained through Eq. (16) from radiative width [17]

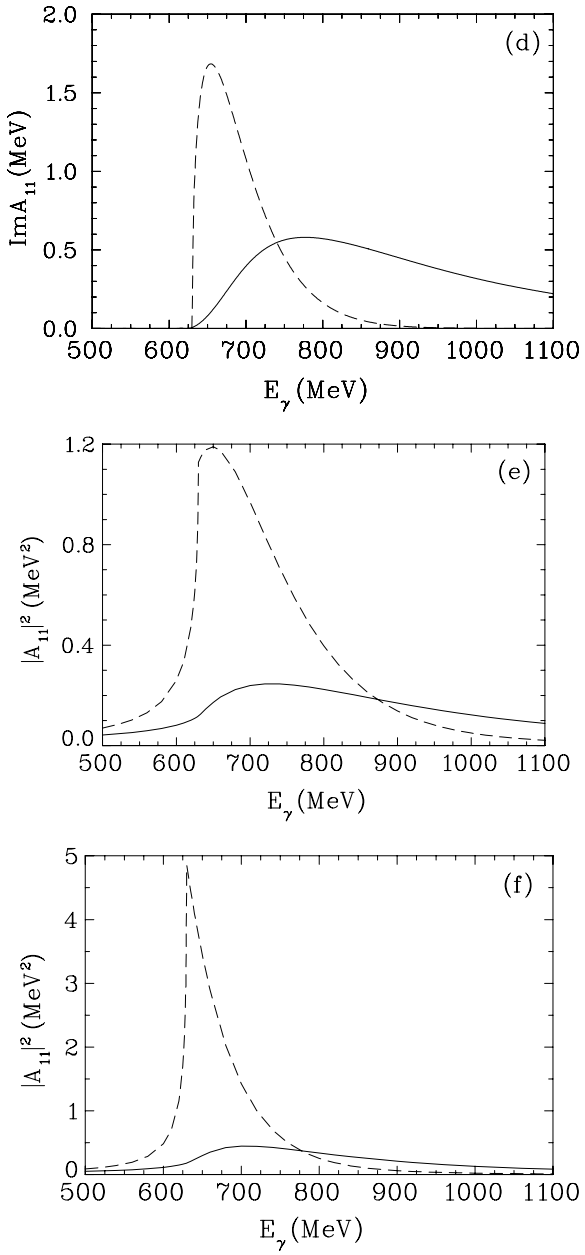

FIG. 5. (*Continued.*)

$$\Gamma_{\omega\to\pi^0\gamma} = 8.7\times 10^{-2}\Gamma_\omega, \qquad \Gamma_\omega = 8.44\ \text{MeV}. \tag{37}$$

The strong coupling constant $g_V = g_{VNN}$ is not well determined, as was mentioned in Ref. [5]. In various analyses, it varies in the range [26,27]$8 < g_\omega < 20$. (We discuss only the vector coupling constants; tensor couplings are neglected according to Sec. II C.) Here, we list some values of g_ω from the aforementioned papers:

$$g_\omega = 21\,[5], \qquad g_\omega = 8\,[4], \qquad \frac{g_\omega^2}{4\pi} = 20\ [20]\ \text{(full model)}. \tag{38}$$

For our subsequent results, we use the value $g_\omega^2/4\pi = 20$ ($g_\omega \approx 15.85$) from Ref. [20].

In Fig. 6, we show the calculated differential cross section of reaction (1) with backward π^0 photoproduction as a function of the photon laboratory energy E_γ at several fixed values of $z = \cos\theta$ from $z = 0$ to $z = -0.85$. (The experimental CLAS data, which are presented in [1], are at the same z values.) The results shown by the solid curves have been obtained with the total amplitude $M_{\gamma d}$ consisting of the terms (22) and (35). The other curves are explained in the figure caption. One can see that the contribution from single-scattering amplitudes dominates the cross section for $z = 0$. The relative contribution from the other amplitudes increases as z approaches -0.85. Note that the ω-exchange amplitude M_ω dominates in the total contribution from single-scattering amplitudes.

TABLE I. $N(1535)$ and $N(1440)$ resonance couplings. Units are $(\text{GeV})^{-1/2}\times 10^{-3}$.

	Ref.	[24]-1	[24]-2	[25]	[11]	[5]	PDG [17]
$N(1535)$	$A^p_{1/2}$	78	50	53	97	67	90
	$A^n_{1/2}$	−50	−37	−98	—	−55	−46
$N(1440)$	$A^p_{1/2}$	−66	−64	−69	—	−71	−65
	$A^n_{1/2}$	50	45	56	—	60	40

In Fig. 6, we see a maximum in the energy spectra of the differential cross section at $E_\gamma \approx 700$ MeV, in the angular region of $z < -0.65$. This maximum gets more pronounced as $z \to -0.85$. The CLAS experimental data [1] also show the excess of events, but less sharp, of the same order of magnitude (increasing as $z \to -0.85$) in a region around the same energy for the same angles. For more detailed discussion, we should mention that the effective energies $\sqrt{s}$ in subprocesses on the nucleons in the double-scattering diagram [Fig. 1(b)] are calculated in the approximation (30). These energies, $\sqrt{s}$, are equal to the ηN-threshold mass at $E_\gamma \approx 700$ MeV. The maxima in Fig. 6 reflect the ηN-threshold effect from the $N(1535)$ propagators in the elementary amplitudes because we use the energy-dependent width $\Gamma_1(s)$ of $N(1535)$ according to Eqs. (11) and $\Gamma_{1\eta}(s) = 0$ at $\sqrt{s} \leqslant m + m_\eta (E_\gamma \leqslant 700$ MeV). The main effect comes from the double-scattering amplitude $M_{1\eta 1}$ with two $N(1535)$ propagators whereas the contribution from $M_{1\pi 1}$ is much smaller owing to a small $N(1535)N\pi$ coupling constant ($g_{1\pi} \ll g_{1\eta}$). Thus, Fig. 6 demonstrates the effects of the two-particle (ηN) threshold in the elementary amplitudes on the intermediate nucleons. At the same time, for the reasons discussed in Sec. III A, we do not see a sizable threshold effect from the three-particle (ηNN) intermediate state ($E_{\text{th}} = 630$ MeV).

Note that the prescription (30) usually works well because of the rapid momentum dependence of the DWF in comparison with ones for the amplitudes of the reactions on the nucleon. However, this approximation does not reproduce adequately any sharp peculiarities of elementary amplitudes in the amplitude of a nuclear reaction. Because of "Fermi motion" within the deuteron, the ηN threshold in the diagrams in Fig. 1 are not positioned at a fixed value of E_γ. These effects tend to be spread over some region of the incoming photon energy. Thus, the sharp maximum at $E_\gamma \approx 700$ MeV in Fig. 6 should be smoothed, but we have no proper simple procedure to do this.

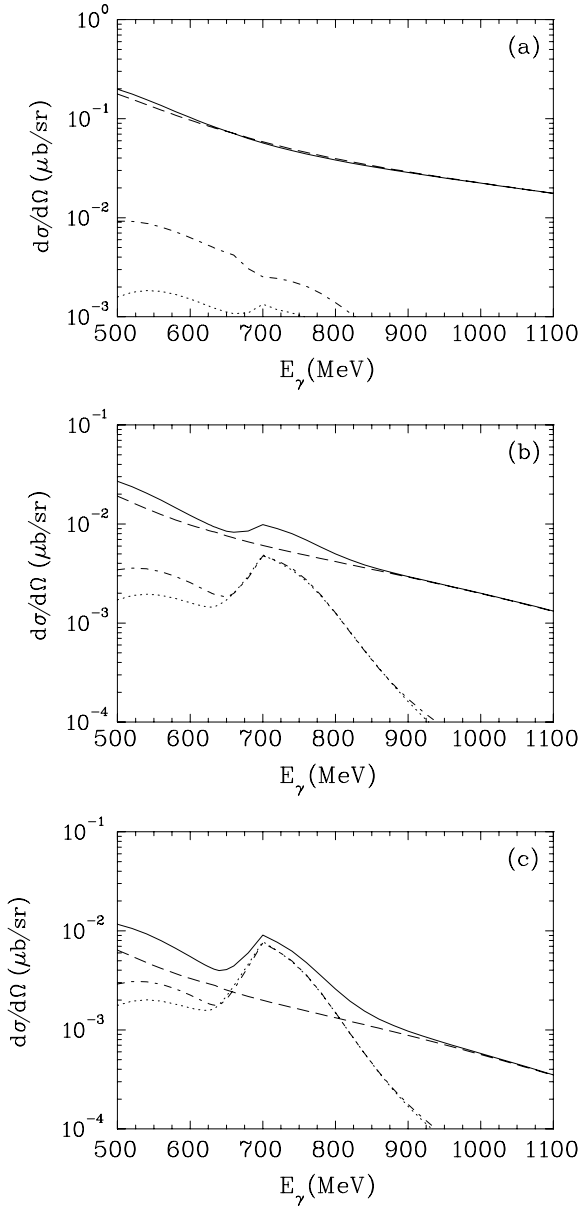

FIG. 6. Differential cross sections of the reaction (1) vs photon laboratory energy E_γ at several values of $z = \cos\theta$. Dashed (dotted) and solid curves show the contributions of single- (double-) scattering amplitudes and total amplitude, respectively. Dash-dotted curves correspond to the contributions of total amplitude without the ω-exchange term. The results are obtained with energy-dependent total width of $N(1535)$. (a) $z = 0$, (b) $z = -0.65$, and (c) $z = -0.85$.

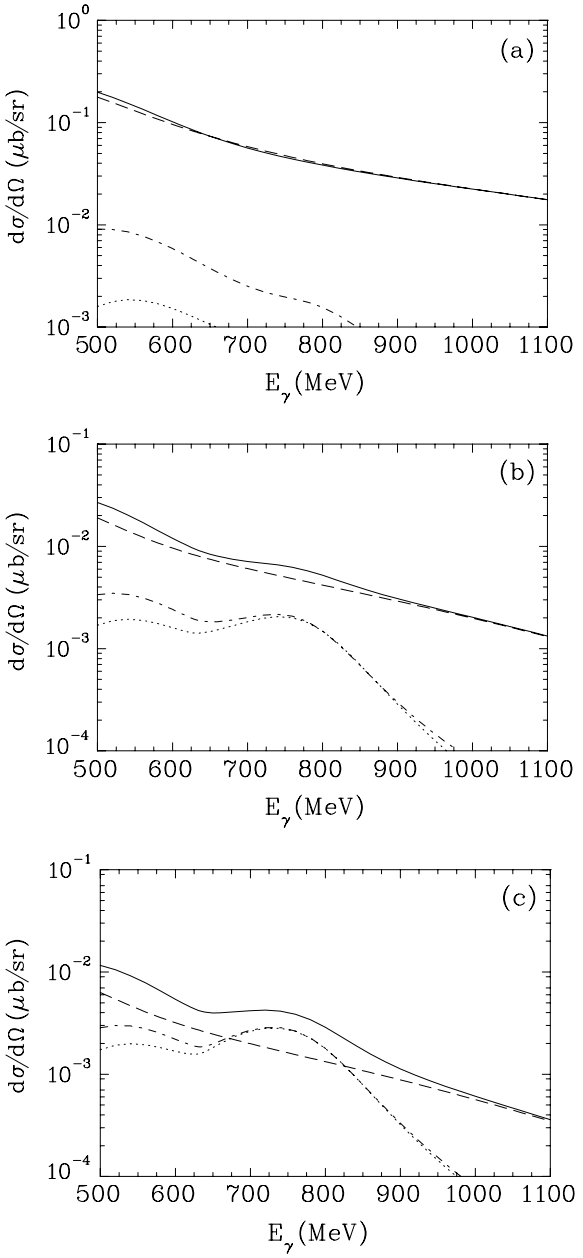

FIG. 7. The same as in Fig. 6 but the results are obtained with constant total width of $N(1535)$.

Let us consider the case when the $N(1535)$ width in the elementary amplitudes is a constant nominal value $\Gamma_1(s) \equiv \Gamma_1 = 150$ MeV. In this case, shown in Fig. 7, we have no ηN-threshold effects in the elementary amplitudes and no sharp maxima at $E_\gamma \approx 700$ MeV. Here, we see broad enhancements centered around $E_\gamma = 750$ MeV. These enhancements appear mainly from the contribution of the amplitude $M_{1\eta 1}$ with two $N(1535)$ propagators. Their position is shifted to the left of $E_\gamma \approx 785$ MeV [laboratory photon energy on the nucleon target with an effective c.m. energy equal to the $N(1535)$ mass] owing to decreasing factors from DWF's in reaction (1). Note that the energy-dependent $N(1535)$ width $\Gamma_1(s)$ at the ηN threshold ($\sqrt{s} = m + m_\eta$), where $\Gamma_{1\eta}(s) = 0$, is about half the size of the nominal value Γ_1 of the $N(1535)$ resonance. Thus, taking $N(1535)$ with constant nominal width, we get smaller values of the corresponding elementary amplitudes in the region close to the ηN threshold. Therefore, the differential cross sections in Fig. 6 at $E_\gamma \sim 700$ MeV are essentially enhanced in comparison with those of Fig. 7. Finally, we conclude that the enhancements in the energy region near the η threshold, shown in Figs. 6 and 7, are mainly due to the $N(1535)$ contributions to the double-scattering diagram with an intermediate η production.

The absolute values of the calculated differential cross section at $z = 0$ [Figs. 6(a) and 7(a)] are in an approximate

agreement with CLAS data [1]. For larger scattering angles θ, our results are lower in absolute value than those of the data. At $z = -0.85$ [Figs. 6(c) and 7(c)], the calculated differential cross sections are considerably smaller than the experimental ones. We expect that the contribution from the single-scattering amplitude M_ω in our treatment is too large. However, adding the VME terms in the double-scattering amplitudes (not included here) may essentially improve our predictions as $z \to -0.85$, where the contribution from the term M_ω gets smaller. Thus, we hope that, by decreasing the elementary ω-exchange amplitude (taking smaller coupling constant $g_{\omega NN}$ and introducing form factors) and including double-scattering amplitudes $M_{\omega\pi 1}$ and $M_{\omega\pi 2}$, we may have a good description of the experimental absolute cross sections at $z = 0$ and essentially improve our predictions as $z \to -0.85$.

IV. CONCLUSION

We considered the energy dependence of the differential cross sections of the reaction $\gamma d \to \pi^0 d$ in a wide energy range around the η-meson photoproduction threshold at several backward c.m. angles of the outgoing pion. Our calculations are based on a nonrelativistic diagrammatical technique and take into account single- and double-scattering amplitudes. We conclude that the contribution of double-scattering with intermediate production of an η meson can explain the structure experimentally observed by the CLAS Collaboration [1] in the energy dependence of the differential cross section near the η threshold. Indeed, our calculations show that a broad enhancement (with width of the order of 100 MeV) appears in the energy behavior of the differential cross section at large scattering angles θ in the η-threshold region. This enhancement becomes more pronounced as θ increases, and the magnitude of the effect is in qualitative agreement with the CLAS data.

We discussed the role of the three-particle $NN\eta$-threshold effect, taking into account "nonstatic" corrections to the η propagator. Indeed, we found that a sharp energy behavior of the differential cross section at the energy of the η threshold calculated in a "static" approximation was essentially smoothed by taking into account "nonstatic" corrections to the η propagator. Our calculation results show that the enhancements in the energy dependence of the differential cross section are, to a great extent, due to the $N(1535)$ contributions in the elementary amplitudes of the double-scattering diagram with intermediate η production.

Our predictions depend on a number of parameters, some of which are not well established (e.g., the constant $g_{\omega NN}$, form-factor parameters, etc.). Not all of the possible diagrams are considered in our analysis. Our calculations do not include VME terms in the double-scattering amplitudes or any other resonance amplitudes besides the $N(1535)$ and $N(1440)$ contributions. Thus, there is room for further improvements of our predictions.

ACKNOWLEDGMENTS

This work was supported in part by Russian RFBR Grant No. 02–02–16465, U. S. Department of Energy Grant DE–FG02–99ER41110, and The George Washington University Center for Nuclear Studies. I. I. S. acknowledges partial support from Jefferson Lab and the Southeastern Universities Research Association under DOE Contract DE–AC05–84ER40150.

[1] Y. Ilieva [for the CLAS Collaboration], Nucl. Phys. **A737**, S158 (2004) [nucl-ex/0309017].
[2] R. L. Walker, Phys. Rev. **182**, 1729 (1969).
[3] R. G. Moorhouse, H. Oberlack, and A. H. Rosenfeld, Phys. Rev. D **9**, 1 (1974).
[4] H. Garcilazo and E. Moya de Guerra, Nucl. Phys. **A562**, 521 (1993).
[5] D. Drechsel, O. Hanstein, S. S. Kamalov, and L. Tiator, Nucl. Phys. **A645**, 145 (1999) [nucl-th/9807001].
[6] P. Bosted and J. M. Laget, Nucl. Phys. **A296**, 413 (1978).
[7] H. Garcilazo and E. Moya de Guerra, Phys. Rev. C **52**, 49 (1995).
[8] S. S. Kamalov, L. Tiator, and C. Bennhold, Phys. Rev. C **55**, 98 (1997) [nucl-th/9602023].
[9] J. M. Laget, Phys. Rep. **69**, 1 (1981).
[10] G. Knöchlein, D. Drechsel, and L. Tiator, Z. Phys. A **352**, 327 (1995) [nucl-th/9506029].
[11] M. Benmerrouche, N. C. Mukhopadhyay, and J. F. Zhang, Phys. Rev. D **51**, 3237 (1995) [hep-ph/9412248].
[12] F. Ritz and H. Arenhövel, Phys. Lett. **B447**, 15 (1999) [nucl-th/9810027]; Phys. Rev. C **64**, 034005 (2001) [nucl-th/0011089].
[13] C. Bennhold and H. Tanabe, Nucl. Phys. **A530**, 625 (1991).
[14] L. A. Kondratyuk and F. M. Lev, Yad. Fiz. **23**, 1056 (1976) [Phys. At. Nucl. (former Sov. J. Nucl. Phys.) **23**, 556 (1976)]; Yad. Fiz. **27**, 831 (1978) [Phys. At. Nucl. (former Sov. J. Nucl. Phys.) **27**, 441 (1976)]; L. A. Kondratyuk, F. M. Lev, and L. V. Shevchenko, *ibid.* **36**, 377 (1982) [Phys. At. Nucl. (former Sov. J. Nucl. Phys.) **36**, 220 (1982)].
[15] B. M. Abramov *et al.*, Nucl. Phys. **A372**, 301 (1981); R. Keller *et al.*, Phys. Rev. D **11**, 2389 (1975); M. Akemoto *et al.*, Phys. Rev. Lett. **50**, 400 (1983).
[16] A. Imanishi *et al.*, Phys. Rev. Lett. **54**, 2497 (1985).
[17] S. Eidelman *et al.* (Particle Data Group), Phys. Lett. **B592**, 1 (2004); [http://pdg.lbl.gov].
[18] R. A. Arndt, W. J. Briscoe, I. I. Strakovsky, and R. L. Workman, Phys. Rev. C **66**, 055213 (2002) [nucl-th/0205067].
[19] V. E. Tarasov, V. V. Baru, and A. E. Kudryavtsev, Yad. Fiz. **63**, 871 (2000) [Phys. At. Nucl. **63**, 801 (2000)].
[20] R. Machleidt *et al.*, Phys. Rep. **149**, 1 (1987).
[21] A. E. Kudryavtsev, V. E. Tarasov, I. I. Strakovsky, W. J. Briscoe, and Y. Ilieva, nucl-th/0408027 (extended version of the present paper).
[22] This "c-transformation" is applied to nucleon spin and isospin operators when writing the expression for the amplitude; we move along the nucleon lines (anticlockwise here) of the diagram in the direction of the nucleon momentum [19].

[23] V. M. Kolybasov and A. E. Kudryavtsev, Yad. Fiz. **17**, 42 (1973) [Phys. At. Nucl. (former Sov. J. Nucl. Phys.) **17**, 22 (1973)].
[24] R. A. Arndt, R. L. Workman, Z. Li, and L. D. Roper, Phys. Rev. C **42**, 1864 (1990).
[25] R. L. Crowford and W. T. Morton, Nucl. Phys. **B211**, 1 (1983).
[26] R. Davidson, N. C. Mukhopadhyay, and R. Wittman, Phys. Rev. D **43**, 71 (1991).
[27] O. Dumbrajs *et al*., Nucl. Phys. **B216**, 277 (1983).